May 2016

Interactions between Inflammatory Cells and CoCrMo Alloy Surfaces under Simulated Inflammatory Conditions

Huiyu Shi
Syracuse University

Abstract

Metallic biomaterials continue to be the primary materials for medical devices because of their excellent physical and mechanical properties especially for certain implants which need high strength (hip, spinal, shoulder, knee etc.). However there is no perfect material to meet all the requirements of a medical device. Metallic biomaterials are prone to corrosion and wear which has been associated with implant failure (osteolysis, aseptic loosening, pseudo tumor etc.) This study focused on investigating how inflammatory cells interact with CoCrMo alloy surfaces under simulated inflammatory conditions (H_2O_2 treatment). It is hypothesized that the presence of Reactive Oxygen Species (ROS) in cell culture will affect the viability of inflammatory cells and that when ROS interacts with CoCrMo alloy surfaces the effect on cell viability is increased. The first part of the study focused on the cell behavior (viability and morphology) when cultured directly on CoCrMo alloy surfaces with different concentrations of H_2O_2 in the medium (0.2 mM – 1 mM) and compared with the same solution conditions but on tissue culture substrate. The electrochemical behavior of CoCrMo alloy surfaces was also examined when exposed to inflammatory cells and inflammatory fluid (i.e. medium with H_2O_2 added). The results show a narrower range of H_2O_2 concentration for cell viability for the CoCrMo group when compared to tissue culture substrate ($p < 0.05$). This indicates that the presence of metal implants during inflammation might raise the ROS toxicity towards cells after surgery. Inflammatory conditions (i.e. H_2O_2 + inflammatory cells) were also found to result in corrosion of CoCrMo alloy surfaces. These short-term results raise significant questions about the long-term interactions between ROS, CoCrMo alloy and inflammatory cells.

Interactions between Inflammatory Cells and CoCrMo Alloy Surfaces under Simulated Inflammatory Conditions

By

Huiyu Shi

B.S. Biological Sciences, Wuhan University, 2010

Thesis

Submitted in partial fulfillment of the requirements for the degree of Master of Sciences (M.S.) in *Bioengineering*

Syracuse University

May 2016

Acknowledgement

I would like to take this opportunity to express my great gratitude to people who encouraged and helped me with my master's work. First and foremost, I want to thank my advisor Dr. Jeremy L. Gilbert for his great patience and guidance. I really appreciate the time and the effort he spent on me explaining every question I had regarding my research project. I learned a lot from him not only the scientific knowledge but also the right attitude of doing research.

I would like to thank Dr. Dacheng Ren, Dr. James H. Henderson, and Dr. Scott Erdman for taking their time to serve on my defense committee.

In addition, I would also like to express my sincere gratitude to Dr. Shiril Sivan. I received lots of help from him about doing experiments in the lab, and he was always willing to help whenever I came across any problems. With his help I could perform my project smoothly. Also I want to thank you all my labmates: Greg Kubacki, Yangping Liu, Zhe Li, and Dongkai Zhu.

Last but not least, I would like to thank all my family members, especially my parents who love me and support me unconditionally in my life. And mostly a great thank you to Jua Kim, who came to my life at the best time and is always there for me no matter good or bad times. It is all your support that I can accomplish this work.

Contents

List of Figures

List of Tables

Introduction

1. Metal implants background

Metals have been widely used for medical devices for many decades. One of the earliest application of a metal implant for medical treatment was discovered by Lane, who used metal plate in 1895 for bone fracture fixation [1]. Since then, metallic biomaterials have been a dominant material used in orthopedic surgery and other medical applications (see Table. 1) [1, 2].

There are many degradation modes associated with metallic materials such as corrosion (fretting and pitting, fatigue), wear, and fracture which can cause implant failure or may induce an adverse local tissue reaction due to the particles & ion release or metallic allergy. Metals are still the best candidate material for many medical device applications because of their good physical and mechanical properties when compared with other materials (see Table 2) [1, 2]. Implant materials require a good combination of strength and ductility which makes metals better candidates than polymers or ceramics. Different metals have been developed to meet the specific needs of certain implant parts. CoCrMo alloy is used for parts which need to have good wear resistance (femoral head of hip implant), Ti-6Al-4V is used for parts that need to have good corrosion resistance and integration with bone (femoral stem of hip implant), and Mg based alloys are being considered for biodegradable implants. Meanwhile different fabrication processes have been developed to make the best use of metal materials (cast, wrought, thermo-mechanical process, powder metallurgy, etc.).

Division	Material	Examples
Cardiovascular	316L SS; CoCrMo; Ti; Ti6Al4V	Stent; Artificial valve
Orthopedic	316L SS; CoCrMo; Ti; Ti6Al4V; Ti6Al7Nb	Bone fixation; Artificial joints
Dentistry	316L SS; CoCrMo; TiNi; TiMo; AgSn (Cu); Amalgam; Au	Orthodontic wire; Filling
Craniofacial	316L SS; CoCrMo; Ti; Ti6Al4V	Plate and screw
Otorhinology	316L SS	Artificial eardrum

Table 1. Different materials for different medical application [1]

Material	Main alloying composition (wt %)	YS (MPa)	UTS (MPa)	YM (GPa)	Max elongation (%)
316L SS (ASTM, 2003)	Bulk Fe; 16-18.5 Cr; 10-14 Ni; 2-3 Mo; <2 Mn; <1 Si; <0.003C	190	490	193	40
CoCrWNi (F90) (ASTM, 2007a)	Bulk Co; 19-21 Cr; 14-16 W; 9-11 Ni	310	860	210	20
CoNiCrMo (F562) (ASTM, 2007b)	Bulk Co; 33-37 Ni; 19-21 Cr; 9-10.5 Mo	241	793	232	50
Pure Ti grade 4 (F67) (ASTM, 2006)	Bulk Ti; 0.05 N; 0.1 C; 0.5 Fe; 0.015 H; 0.4 O	485	550	110	15
Ti6Al4V (F136) (ASTM, 2008)	Bulk Ti; 5.5-6.75 Al; 3.5-4.5 V; 0.08 C; 0.2 O	795	860	116	10

Table 2. Example of metal/metal alloy mechanical properties [1]

Even though many metal implant improvements have been discovered over the past several decades, there are still significant problems associated with metal devices. As the use of artificial implants increases year by year worldwide, the failure of implants has become more and more significant. The complexity of interactions between metals and physiological

environment has not been well understood by scientists to date. Basically, there are two perspectives of studying metal implants and the biological system, one is how implants affect the body and the other is how body affects the metal implants.

2. Biological system

When considering the impact of metal implants on the body, it raises the concept of "biocompatibility". Biocompatibility is defined as "the ability of a biomaterial to perform its desired function with respect to a medical therapy, without eliciting any undesirable local or systemic effects in the recipient or beneficiary of that therapy, but generating the most appropriate beneficial cellular or tissue response in that specific situation, and optimizing the clinically relevant performance of that therapy" [1, 2]. Based on this concept, there is no metal that is perfectly biocompatible as an implant material. Even Ti and Mg, which are thought of as biocompatible to the living body, have some adverse effects on the biological system. During cyclic micro-motion (which is inevitable among modular metal implants), the metal implant's potential may drop to as low as -1 V, and studies have shown preosteoblasts were dead when cultured on Ti surface under negative voltages (-600 mV and -1 V) [3]. Meanwhile it has also been shown that Mg particles can also kill preosteoblasts [4]. While many studies have shown that Ti and Mg ions are not toxic to living body, it is therefore interesting to investigate what causes the cell death.

One hypothesis for negative potential killing cells is that extra electrons accumulate on the metal surfaces and react with water molecules to create reactive oxygen species (ROS) (most

commonly H_2O_2), which is toxic to living cells [5]. Another hypothesis of Mg particles killing cells is similar in that during Mg particle corrosion, ROS might be generated due to the reduction half-cell reaction which then kills the cells adjacent to particles [4].

ROS are chemical species which include intermediates of oxygen reduction which are highly reactive and strong oxidizing agents. Examples include peroxides, superoxide, hypochlorous acid, and hydroxyl radical [6]. In the living body system, ROS is present and can be formed from normal metabolism of oxygen. Its role is important in many biological activities such as in cell signal transfer and in inflammatory reactions [7]. Especially when there is a wound created in the living body or infection, the concentration of ROS can increase dramatically (post-surgery of implantation). During the wound healing process and inflammation, ROS plays a very important role in signal transfer, cleaning up debris, and in cell proliferation [7, 8]. ROS is generated during respiratory burst associated with phagocytic cells of the body. So when studying metal implants *in-vitro*, it is important to consider the impact of ROS and the interactions of corrosion and inflammation. As shown in Fig.1, three factors: metal implants, cells, and ROS should all be considered when studying the interactions of living systems with metal implants. Therefore, because ROS can be generated both by implant surfaces and by phagocytes, there is a complex interplay between metal surfaces and the biological system and inflammation.

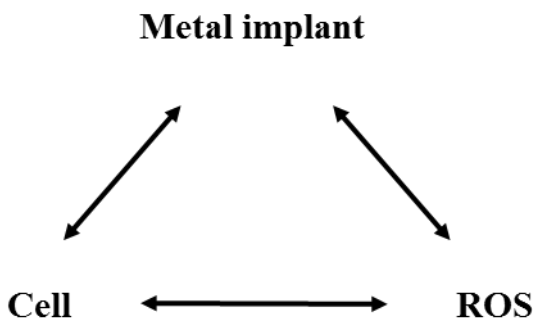

Figure 1. Schematic of the relationship between implant, cell, and ROS.

In the current study, U937 cells were used because of their macrophage-like behavior [9]. After implantation surgery, monocytes migrate into the tissue around implants and differentiate into macrophages and these cells will live months compared to neutrophils which are short-lived only for several days [10]. So it is important to study the interactions of macrophages and metal implants since they can have a long-term impact on each other. Macrophages, once they are activated, will phagocytose foreign bodies. Especially for metal implants, the process of phagocytosis will be different depending on the size of particles. For particles with a diameter of ~2-3 μm or smaller, macrophages can engulf the whole particle and form vesicular bodies full of acids, peroxides, and cytokines for degradation of particles [10]. On the other hand, if particle sizes are bigger than 3 μm, macrophages will try to spread their membrane or they will fuse together to create multinucleated foreign body giant cells to fully cover the surface forming isolated spaces with all kinds of chemicals for degradation process (Fig.2).

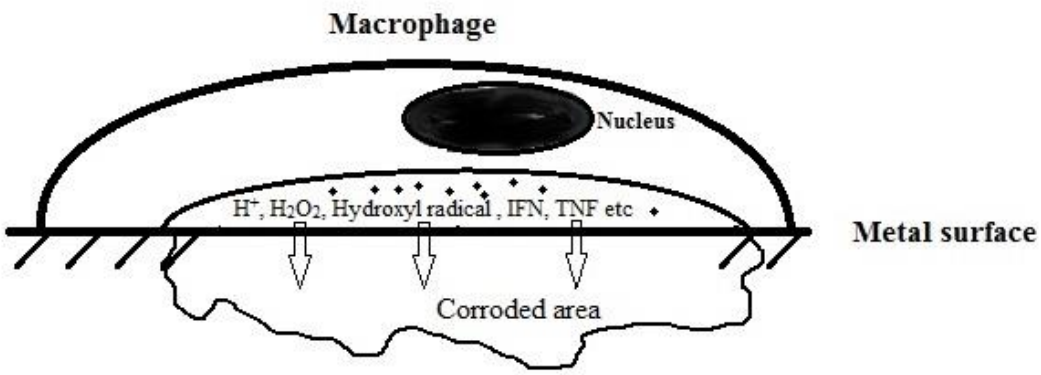

Figure 2. Schematic figure of macrophage induced corrosion.

The U937 cell line was originated from the pleural effusion of a 37 year old male patient with histiocytic lymphoma, and is a monocyte which can differentiate to macrophage-like cells with phorbol 12-myristate 13-acetate (PMA) treatment. PMA can trigger the U937 cells line to produce H_2O_2 and $O_2^{\bullet-}$ even though the capacity for producing these species is weak [9, 11, 12]. U937 cells can partly mimic how macrophages behave *in-vivo* while interacting with metal implants. During inflammation, ROS concentration may vary with different situations, it is like a "double-sides sword" towards living system, and a low dose of ROS is important for cell signaling and can help cell proliferation while high dose of ROS will cause cell death [5].

In the early stage of inflammation, ROS will be generated by inflammatory cells against bacteria, particles, and other foreign bodies to clean the wounded tissue. For low ROS concentrations, it can help improve the functioning of macrophages [13, 14]. However when ROS concentration raises to a high level, it will start to show cytotoxicity to macrophages which is called oxidative stress. So whether ROS will be positively helping or negatively damaging to the living system

depends on its concentration. For all the ROS, H_2O_2 is the most common peroxide in the living system, it can serve as messenger, guide, or assassin during inflammation reactions [7]. Even within healthy conditions, H_2O_2 is necessary to play a role in maintaining cell proliferation and for some cases H_2O_2 can suppress cell death by different mechanisms (degrading H_2O_2 or suppressing H_2O_2) [15, 16]. High H_2O_2 concentration will be toxic and induces different cell death mechanisms (≤ 1mM apoptosis, ≥1mM necrosis) [17, 18]. Therefore it is important to know how cells behave under different H_2O_2 concentrations in order to reveal the mechanism of inflammation.

Even though metallic biomaterials may be the best candidates for many medical devices, severe problems have been discovered after implantation in some cases. The most common failure is thought to be because of metal release (ions and particles) from implant surfaces [19]. CoCr based alloys are often used, however, they are not as biocompatible as Ti based alloys. Cr (VI) is classified as group 1 carcinogen, Cr (III) is classified as group 3 carcinogen, and Co (II/III) is classified with its compounds as group 2B carcinogen [21, 22]. However on the other hand, Cr and Co are important microelements for living system functions, for example Cr plays a role in glucose metabolism and Co (III) is important for activities of vitamins (B12) [22]. Only when their concentrations are in trace quantities they won't show harm to biological targets. The toxicity of Cr or Co is mainly based on their concentrations and the studies of metal implant failure showed significant amounts of metal wear debris and corrosion products around periprosthetic tissues as well as significant amounts of macrophage infiltrate [22]. Macrophages play a vital role in corrosion related implant failure. Evidence of cell induced corrosion was recently hypothesized by Gilbert et al. where cell-like corrosion patterns were found on the

surface of retrieved CoCrMo hip implants [23]. Therefore, as with mechanically assisted corrosion which is well known as cause of implant failure, cell induced corrosion may significantly impact metal implant failure.

3. Fenton reactions in biological system

In the 1890s, H.J.H. Fenton first reported Fe (II)-H_2O_2 system showed strong oxidative effects to organic acids in his paper "Oxidation of tartaric acid in presence of iron" [6]. Later research discovered hydroxyl radical (HO•) can be produced through Fenton reactions and it is detrimental to biological macromolecules such protein, lipids, DNA, etc. [6]. Since iron ions are ubiquitous in the living systems and H_2O_2 is also commonly produced either though metabolism of O_2 or secreted by cells to balance the oxidative state. Without control, detrimental amounts of HO• will be produced to harm the living system. Fortunately for the living system, there are proteins that can combine with metal ions and ion tunnels on cell membrane to control the ion levels in the living system. The living system can properly manipulate how much ROS may be produced either for foreign body clearance or cell signaling.

$$Fe^{2+} + H_2O_2 \rightarrow Fe^{3+} + HO\bullet + HO^- \quad \text{(Reaction 1)}$$

$$Fe^{3+} + O_2\bullet^- \rightarrow Fe^{2+} + O_2 \quad \text{(Reaction 2)}$$

Besides the well-known Fenton reactions which are mediated by iron ions, other transition-metal ions such as Cr^{3+}/Cr^{6+} can also drive the Fenton-like reactions from H_2O_2 to HO• [6]. For CoCr or Ti based alloys, since they are all transition metals, it is important to consider their ability of driving Fenton-like reactions to form HO• and damaging organic macromolecules.

4. Electrochemical testing techniques

In this study, electrochemical tests were performed that include open circuit potential (OCP) versus time, electrochemical impedance spectroscopy (EIS), and atomic absorption spectroscopy (AAS). Voltage, impedance and ion concentration data were collected for the range of H_2O_2 concentrations.

OCP of metal implants indicates the resting potential of metal when there is no net current flow (i.e. where oxidation currents equal reduction currents). Voltage below OCP usually indicates reduction currents are higher than oxidation currents while voltage above OCP indicates oxidation currents are higher than reduction currents. And oxidation currents come from reactions of metal to metal ions or metal oxides while reduction currents usually come from reactions of oxygen to hydroxide ion.

Electrochemical impedance spectroscopy (EIS) tests are used to measure the material surface electrical properties as a function of frequency. Metal implant surfaces have passive oxide films which can serve as both a high resistor and a capacitor-like element, CPE (constant phase element). The impedance of metal surfaces can be written as equation 3. Within all the equations, Z stands for impedance; i is the imaginary number that $i^2 = -1$; R is resistance; C is capacitor; ω is angular frequency which $\omega = 2\pi f$; α stands for exponent for CPE and $\alpha = 0$ means pure resistor behavior while $\alpha = 1$ means pure capacitor behavior; Q is charge quantity.

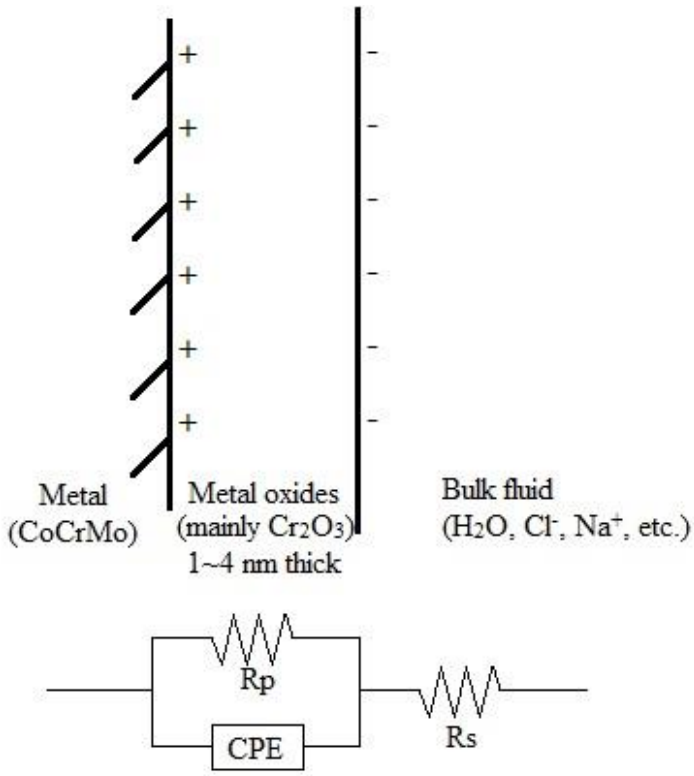

Figure 3. Schematic of electrical double layer and Randle's circuit

$Z = Z' + iZ''$ (Equation 1)

$Z(R) = R; Z(C) = -\frac{1}{i\omega C}; Z(CPE) = -\frac{1}{(i\omega)^{\alpha}Q}$ (Equation 2)

$Z(Total) = Rs + Z,; \frac{1}{Z,} = \frac{1}{Rp} + \frac{1}{Z(CPE)}$ (Equation 3)

Technically the higher the impedance value, the better corrosion resistance of metal implants. For intact metal oxide surfaces, α value should be close to 1 and any changes of α value might indicate defects in the metal oxide film which means poor corrosion resistance. The most common model used to mimic metal surface electrical behavior is the Randle's circuit (Fig 3). Rp stands for the polarization resistance of the metal, Rs stands for solution resistance and CPE mimics imperfect capacitor behavior of metal oxide film.

Besides the Randle's circuit model, there are other more complicated electrical circuit models such as the defective coating model and the crevice impedance model. These two models might more accurately mimic the electrochemical system regarding modular metal implant products, depending on the specific geometry involved.

Atomic absorption spectroscopy (AAS) is used to quantitatively determine chemical elements (most common in solutions) from the absorption of specific light wavelength by gaseous atoms. However this technique cannot detect the valence of elements. The basic theory of this technique is that when different atoms are heated into a gas plasma state, they will absorb specific wavelengths of light which can be measured. Usually AAS techniques can detect element concentrations as low as ~5 μg/L or less. It is very useful to study metal ion release from implants into physiological fluid both *in-vitro* and *in-vivo*.

Study Goals

The goal of this study is to understand the relationship between CoCrMo alloy surfaces, ROS molecules (H_2O_2 in medium solution) and U937 macrophages. It is hypothesized that there is a 3-way synergistic effect of each element of this system on the other. That is H_2O_2 + CoCrMo alloy will have a greater effect on cell viability than either alone and that H_2O_2 + cell will adversely affect corrosion of CoCrMo alloy.

Aims

- Investigate inflammatory cell (U937) viability under oxidative stress (H_2O_2 concentration from 0.2 mM to 1 mM) and compare the viability difference between culturing on plastic substrate and on CoCrMo alloy disc;
- Study the morphology of inflammatory cell (U937) and CoCrMo alloy surfaces after H_2O_2 treatment by digital optical microscope and SEM;
- Investigate electrochemical behavior (OCP, impedance, and ion release) of CoCrMo alloy disc under inflammatory conditions and inflammatory cells (U937).

Materials and Methods

1. Chemical chamber preparation

Metal discs made of Cobalt-Chromium-Molybdenum alloy (ASTM F-1537) were prepared through sequential wet sanding to a 600 grit finish, and then mirror-like polish was performed with 1μm alumina suspension in water. Then the discs were rinsed in deionized water, ultrasonically cleaned in 70% ethanol for 30 minutes, autoclaved for 1 hour 40 minutes, and then exposed to UV light for about 1 hour before use.

A custom made glass electrochemical cell culture chamber [3] was used for testing. As shown in Figure 4, a metal rod was connected to the underside of the CoCrMo disc and passed through the threaded plastic bushing to provide external electrical contact to the disc sample. When the glass chamber was threaded onto the plastic bushing, an O-ring was compressed providing a water tight seal around the CoCrMo surface. This setup exposed approximately 3.8 cm^2 of the disc sample to the interior of the chamber. The chamber was sealed at the top end with a rubber plug with access holes for air exchange, graphite rod counter electrodes, and Ag/AgCl reference electrodes (merged in agar/PBS). The CoCrMo discs served as the working electrodes which constituted a 3-electrode system. All the chamber components were cleaned with Alcotab (Alconox Inc) solution, rinsed with deionized water and autoclaved for 1 hour 40 minutes before mounted together.

To make the Ag/AgCl reference electrode, approximately 5 inches of silver wires (A-M Systems) was cut and a Bunsen burner was used to remove silver oxides and other chemicals on the surface. Then, the wire was wiped with 70% ethanol, coiled at one end, and immediately immersed into bleach for 15 minutes to form AgCl on the silver wire surface. The reference electrode was then rinsed with PBS solution before being put into the cell culture medium.

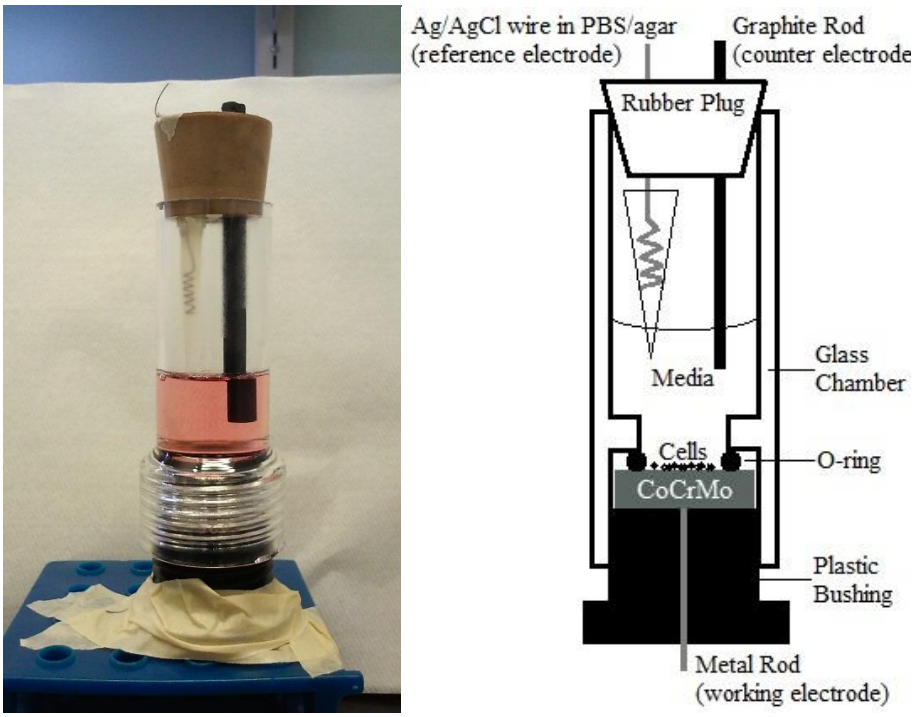

Figure 4. Photo and schematic of electrochemical culture chamber.

2. Cell culture and differentiation

In all experiments, U-937 human histiocytic lymphoma monocyte cell line (ATCC® CRL-1593.2™) was cultured in the RPMI-1640 medium (Gibco) supplemented with 10% (v/v) fetal bovine serum (FBS, Gibco) to make the complete culture medium. Cells were cultured in a T-75 culture flask (Corning, NY) at 37°C, under 5% CO_2 in a humidified atmosphere. The cells were counted with a hemacytometer (Sigma-Aldrich) to achieve the appropriate cell seeding concentration of around 3.5 million cells in 10 ml of medium. For each chamber, 20,000 cells were seeded on a CoCrMo disc surface to make the density of about 5,300 cells/cm^2.

Phorbol 12-myristate 13-acetate (PMA) also known as 12-O-Tetradecanoylphorbol-13-acetate (TPA) was purchased from EMD Millipore. The PMA powder was dissolved in dimethyl sulfoxide (DMSO, Sigma-Aldrich) to make the concentration of 10 mM, stored in Eppendorf PCR tubes, 5 µl each at -20°C. The PMA dosage in all the experiments was 0.7 µl in 30 ml culture medium (233 nM). For each test, before treating cells with H_2O_2, they were differentiated by PMA for 24 hours into macrophages on CoCrMo disc surface.

3. Experimental group design and data acquisition

3.1. Cell viability experiment

In this experiment, cell viability was measured under varying H_2O_2 (Sigma-Aldrich) concentrations for cells seeded on CoCrMo disc surfaces or on tissue culture plastic substrate (6-

well plate, Corning, NY). Table 3 shows the experimental groups. Since the H_2O_2 product was in (wt. %), it is necessary to convert into (mM) to make the calculation easier for each test group. It is known that ρ (H_2O_2) = 1.45 g/ml, ρ (H_2O) = 1 g/ml, ρ (30 wt. % H_2O_2) = 1.11 g/ml, M_w (H_2O_2) = 34 g/mole, M_w (H_2O) = 18 g/mole. From these constants, 30 wt. % H_2O_2 concentration was then calculated to be 9800 mM.

Groups	**H_2O_2 Concentration (mM)**									
Disc	0	0.2	0.3	0.4	0.5	0.6	0.7	0.8	0.9	1
6-well Plate	0	0.2	0.3	0.4	0.5	0.6	0.7	0.8	0.9	1

Table 3. Groups for cell viability test (each concentration group was performed at least three times, n=3).

For each independent test (n=3 for each group), besides H_2O_2 concentration, other conditions were kept constant: 20,000 cells seeded on disc surfaces or 6 well plates with 5 ml fresh media; before 24 hours of different H_2O_2 concentrations treatments, all groups were treated with PMA for 24 hours for cell differentiation.

Cell viability on CoCrMo disc and 6-well plate were assessed using Live/Dead® Viability/Cytotoxicity Kit for mammalian cells (SKU# L-3224, Invitrogen). After H_2O_2 treatment, cells were washed with PBS then incubated at room temperature with a solution containing calcein and ethidium homodimer-1 in PBS for 25 minutes. For disc samples, they were first transferred to 6-well plate and then washed with PBS gently. The dye solution used

for each well and disc was 150 µl, and it was kept from light when performing the experiment. Table 4 shows the components of dye solution.

Chemicals	Volume (µl)
PBS	300
Calcein	0.1
Ethidium homodimer-1	0.8

Table 4. Live & Dead fluorescent assay dye volume for test.

For image processing, cells were imaged with an inverted microscope (Axiovert 40CFL, Zeiss, Denmark) equipped with a CCD mono-12 bit camera (Q-imaging, Canada) and an X-cite 120 light source (EXFO America, TX). Live cells (green) were imaged using fluoroscien bandpass filter and dead ones (red) were imaged by Texas red dye filter. The software Image-Pro 3D suite version 5.1 (Media Cybernetics, Md) was used to acquire and overlay the live (green) and dead (red) images. For 6-well plate groups, it is easy to take pictures under the microscope, however for discs groups, the excess solution on samples were first blotted off with Kim-wipes and then placed inverted on a petri dish with glass coverslip spacers to prevent squeezing cells for imaging. Eight pictures were taken for each sample from random positions. ImageJ software (NIH) was used for live and dead cell counting. Equation 4 was used for cell viability calculation.

$$Cell\ Viability\ \% = \frac{\#\ of\ live\ cells}{\#\ of\ live\ cells + \#\ of\ dead\ cells} \quad \text{(Equation 4)}$$

3.2. Electrochemical experiment

The open circuit potential (OCP), electrochemical impedance spectroscopy (EIS), and atomic absorption spectroscopy (AAS) tests were performed. Table 5 shows all the experimental groups. These test were carried out for each group in each test (n=3).

Groups	**H_2O_2 treatment**
Media control	0
Media + H_2O_2	0.25 mM
Media + H_2O_2	1 mM
U937 cell control	0
U937 cell + H_2O_2	0.25 mM

Table 5. Groups for electrochemical test (at least three samples were tested for each group, n=3). All groups were performed for 24 hours.

Data were acquired by a potentiostat (Solartron 1280C, UK) equipped with a frequency analyzer. For each group, before H_2O_2 treatment, OCP data of CoCrMo disc was first collected via Corrware 2.0/Corrview 2.0 software (Scribner Associates) for 15 minutes until the potential was relatively stable.

EIS measurement was performed by superimposing a 10 mV sinusoidal voltage at OCP vs. Ag/AgCl with scanning frequency from 20,000 Hz to 0.01 Hz. Zplot 2.0/Zview 2.0 software (Scribner Associates) was used to acquire and analyze the impedance data. After adding H_2O_2 to culture medium, the change in OCP was measured and compared to the potential data prior to

H_2O_2 introduction. After H_2O_2 treatment for 24 hours, another set of OCP and EIS tests were performed as before to compare with the former data.

AAS data were acquired by Zeeman Effect Atomic Absorption Spectrophotometer (Model 170-70). Table 5 shows each tested group. In this experiment, supernatant media samples were stored in -80℃ freezer after each electrochemical test for later AAS testing. Before testing, standard element concentrations were made to calibrate the machine and standard line of ion concentration vs voltage data was then calculated. A LabVIEW ™ program was used to acquire the voltage output signal.

3.3. Cell and disc surface morphology analysis

After a total of 48 hours in culture, all the chamber components were disassembled and the CoCrMo disc samples were rinsed with PBS to remove the non-adherent cells. Then fixed with 4% formaldehyde in PBS for 2 hours and dehydrated with graded ethanol PBS mixtures: 50%, 75%, 90% and 100%, 15 minutes for each gradient. After dehydration, samples were held at 50 mTorr overnight to keep dry from moisture. Digital optical microscope (Hirox 8700, Hirox, Inc. Mahwah, NJ) and Scanning electron microscopy (SEM, JEOL 5600, JEOL, Dearborn MA) were used to observe the details of both cells and disc surfaces, imaging methods included both secondary electron emission (SEI) and backscattered electron mode (BEC). Low kV (4 kV) was

used for cell morphology imaging, while high kV (15 kV) used for disc surface imaging and high kV BEC revealed compositional information of the surface.

3.4. Statistical analysis

Results are shown as means ± standard deviation (SD). Two way ANOVA (SPSS) method was performed, along with post hoc Tukey tests to compare control and H_2O_2 treatment groups as a function of concentration both on 6 well plate and CoCrMo disc with P value of 0.05 indicating a significant difference. All the plots were performed by Microsoft excel worksheet. For each group, at least three independent tests were performed.

Results

1. Cell viability and morphology

Figure 5 demonstrates the U937 cell viability data after 24 hours H_2O_2 treatment. Cells were cultured both on CoCrMo disc and tissue culture plastic and the differences of viability were compared. The result shows that with the increase of H_2O_2 concentration, cell viability decreases, and when H_2O_2 concentration reaches 1 mM, all cells were dead for both conditions. Statistical analysis shows there is a significant difference of viability value between cells cultured on CoCrMo disc and cells cultured on tissue culture plastic ($p < 0.05$). The CoCrMo disc groups resulted in greater killing effect at similar H_2O_2 concentrations. And the plot shows the LD_{50} concentration of H_2O_2 for 6 well plate group is 0.9 mM while for CoCrMo group is 0.8 mM.

Florescent images of U937 cells under different H_2O_2 concentrations (Fig. 6) show nearly all the cells were alive in control group and 0.2 mM H_2O_2 treatment group. Cells with pseudopodia morphology (Fig. 8) were evident under some conditions and a percentage summary of cells with pseudopodia under different conditions are also shown in figure 8. Statistical analysis shows more cells grew pseudopodia morphology when treated with 0.2 mM H_2O_2 compared to control group or 0.3 mM H_2O_2 treatment group. When H_2O_2 concentration reaches to 0.8 mM, nearly half of the cells were dead and all cells were dead in 1 mM H_2O_2 treatment group according to picture (d) and (h) in Fig. 6.

The total number of cells vs. H_2O_2 concentration was plotted in Fig 7, solid lines are from cells on 6 well plate and dashed lines are from cells on CoCrMo disc, and green lines represent the number of live cells while red lines represent the number of dead cells. The plot shows the number of dead cells is similar between 6 well plate group and CoCrMo disc group, but the number of live cells is lower for CoCrMo disc group when compared to 6 well plate group.

More detailed cell morphology images were revealed by SEM techniques which are shown in figure 9. Low kV (4 kV) energy were used to investigate the cell morphology, and cells in the control group were compared with cells in 1 mM H_2O_2 treatment group. The result shows that cells in control group (Fig. 9(a) and 9(b)) had smooth and intact membrane structure and they were actively communicating with each other. In 1 mM H_2O_2 treatment group (Fig. 9(c) and 9(d)), cells were dead in two different mechanisms based on the morphology: apoptosis and necrosis. Necrotic cell shows a broken membrane feature and an indentation on the cell surfaces. Apoptotic cell shows typical apoptotic bodies forming on the cell surfaces.

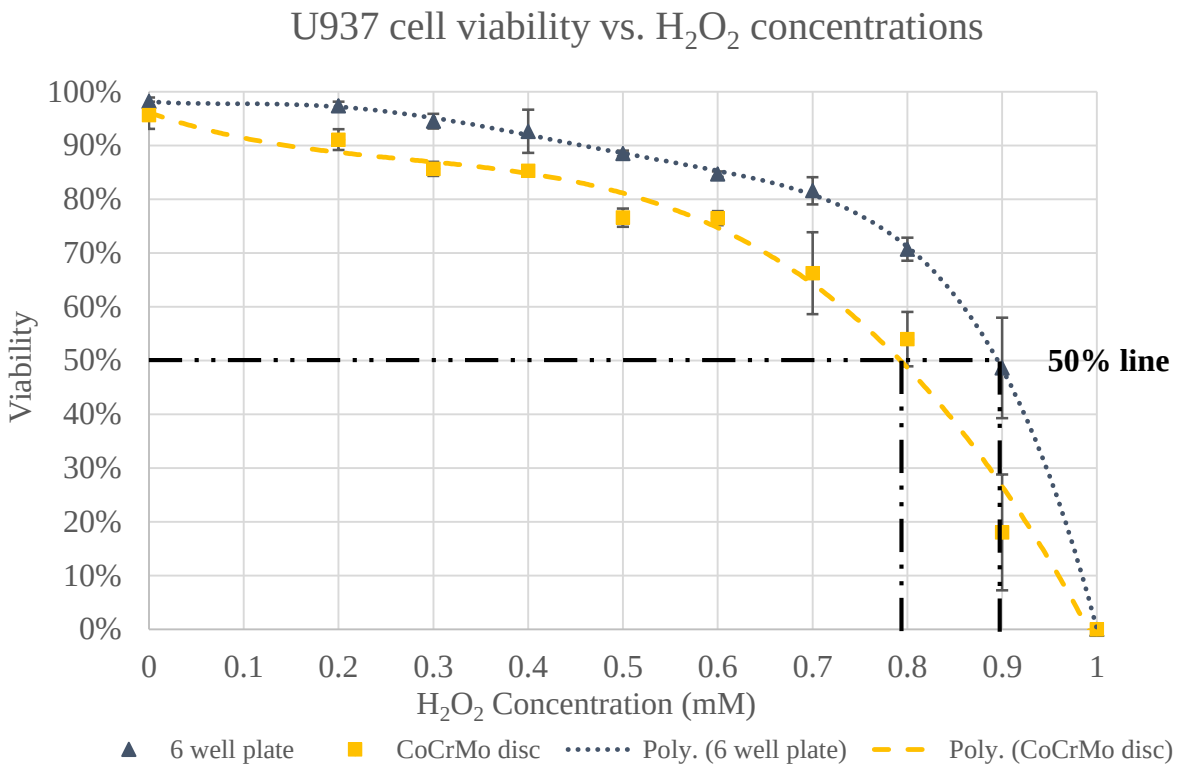

Figure 5. U937 cell viability results after 24 hours H_2O_2 treatment, for cells cultured on 6 well plate and CoCrMo disc showed a significant difference of viability ($p < 0.05$).

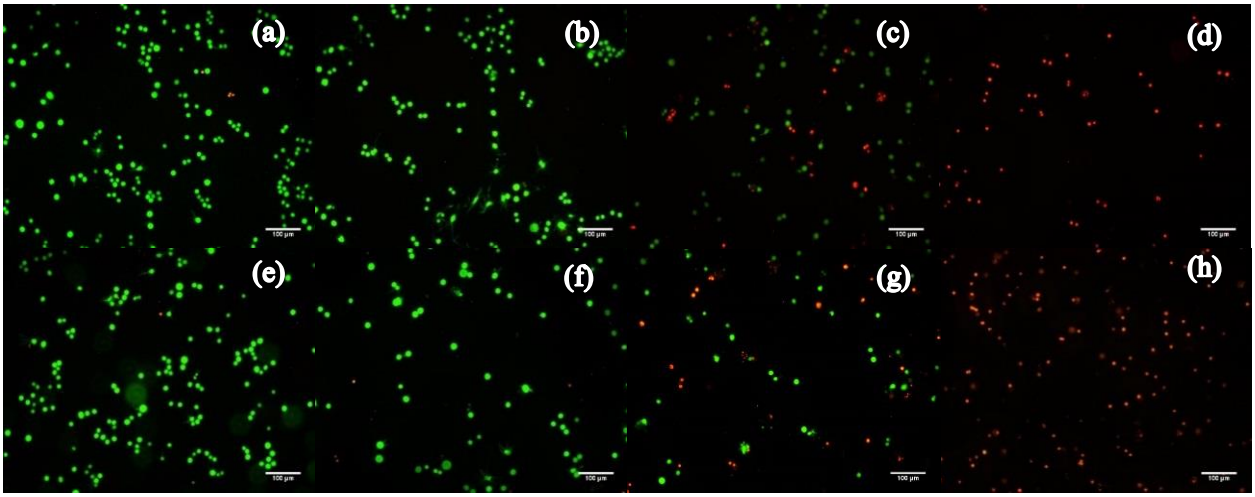

Figure 6. Fluorescent images of U937 cells show the effect of different H_2O_2 concentrations and exposure to CoCrMo after 24 hours. Picture (a) – (d) are cells on 6 well plate and picture (e) – (h) are cells on CoCrMo alloy disc. Picture (a) and (e) are control groups. Nearly all cells were

alive and some even showed pseudopodia morphology. Picture (b) and (f) are 0.2 mM H_2O_2 treatment groups. Picture (c) and (g) are 0.8 mM H_2O_2 treatment groups. Picture (d) and (h) are 1 mM H_2O_2 treatment groups. These pictures demonstrate the differences of viability and morphology of U937 cells under a range of H_2O_2 concentrations.

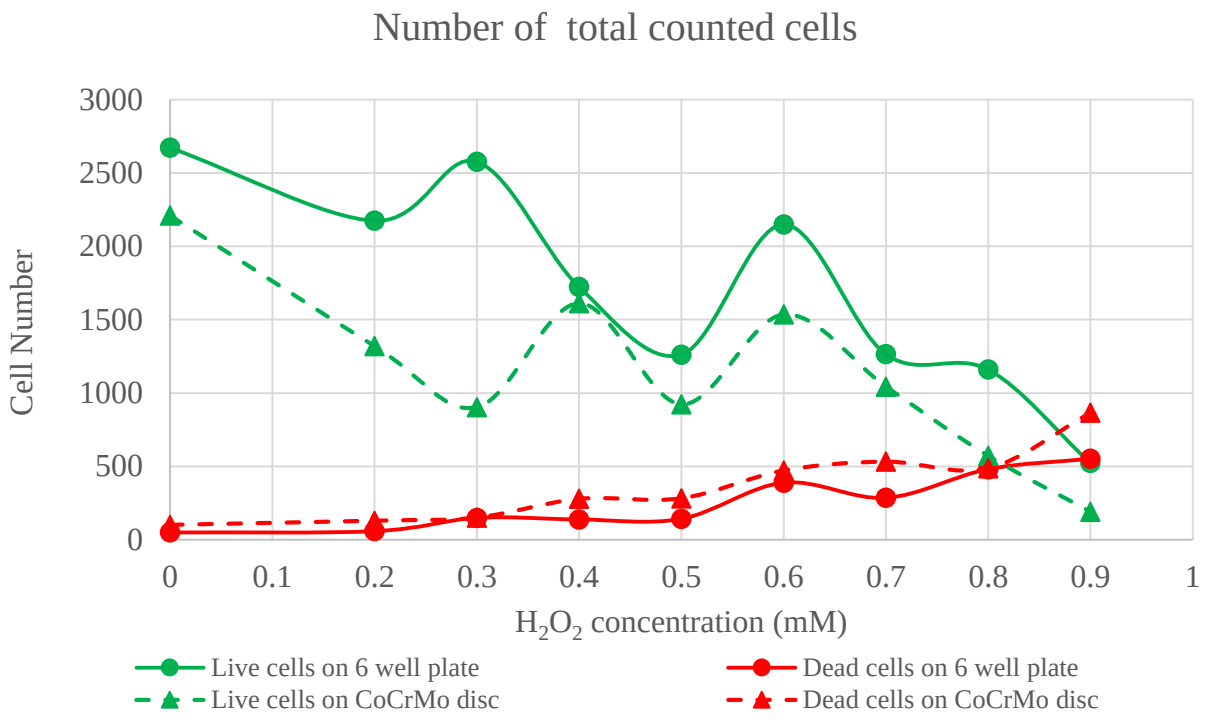

Figure 7. Number summary of counted cells vs. H_2O_2 concentration. The green lines represent live cells and red lines represent dead cells; solid lines represent cells on 6 well plate and dashed lines represent cells on CoCrMo disc.

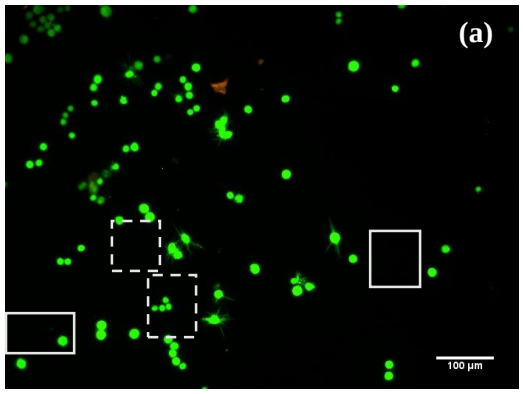

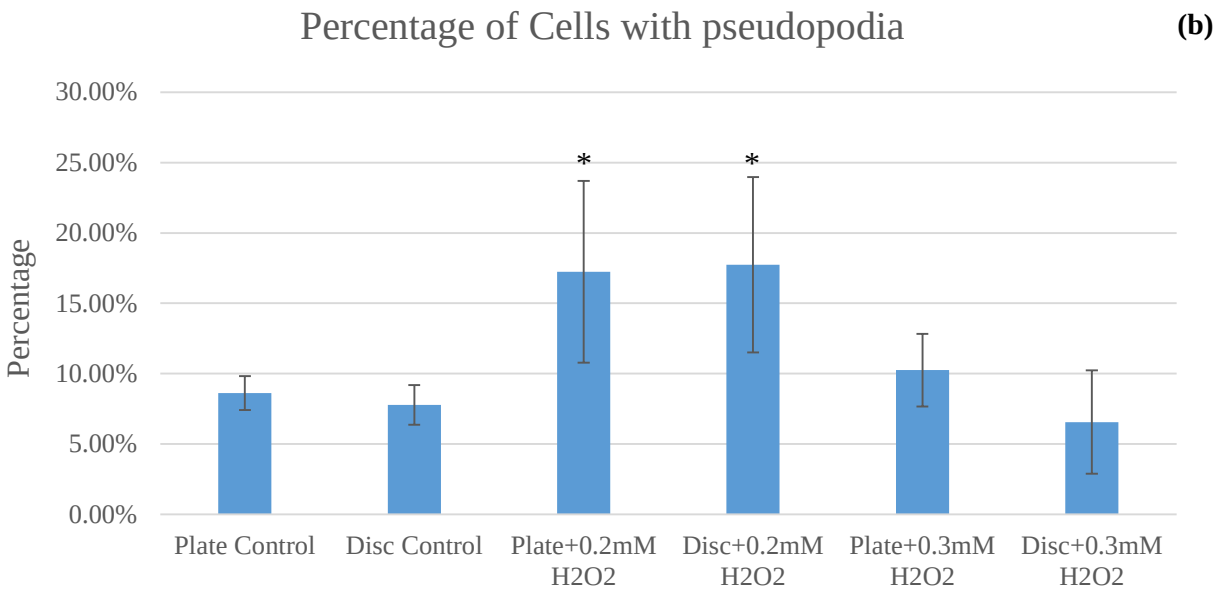

Figure 8. Fluorescent image and percentages of U937 cells with/without pseudopodia show the effect of H_2O_2 treatments with and without CoCrMo. Cells within dashed line area in image (a) were counted as cells with pseudopodia, while cells within solid line area were counted as cells without pseudopodia. Chart (b) shows the summary of pseudopodia cell percentages over all live cells in control group, 0.2mM H_2O_2 treatment group, and 0.3mM H_2O_2 treatment group (24 hours treatment). Two way ANOVA (SPSS) analysis showed no difference between the two different substrates but there is a difference between different H_2O_2 concentration groups. More cells in 0.2mM H_2O_2 group developed pseudopodia indicating more cells were activated.

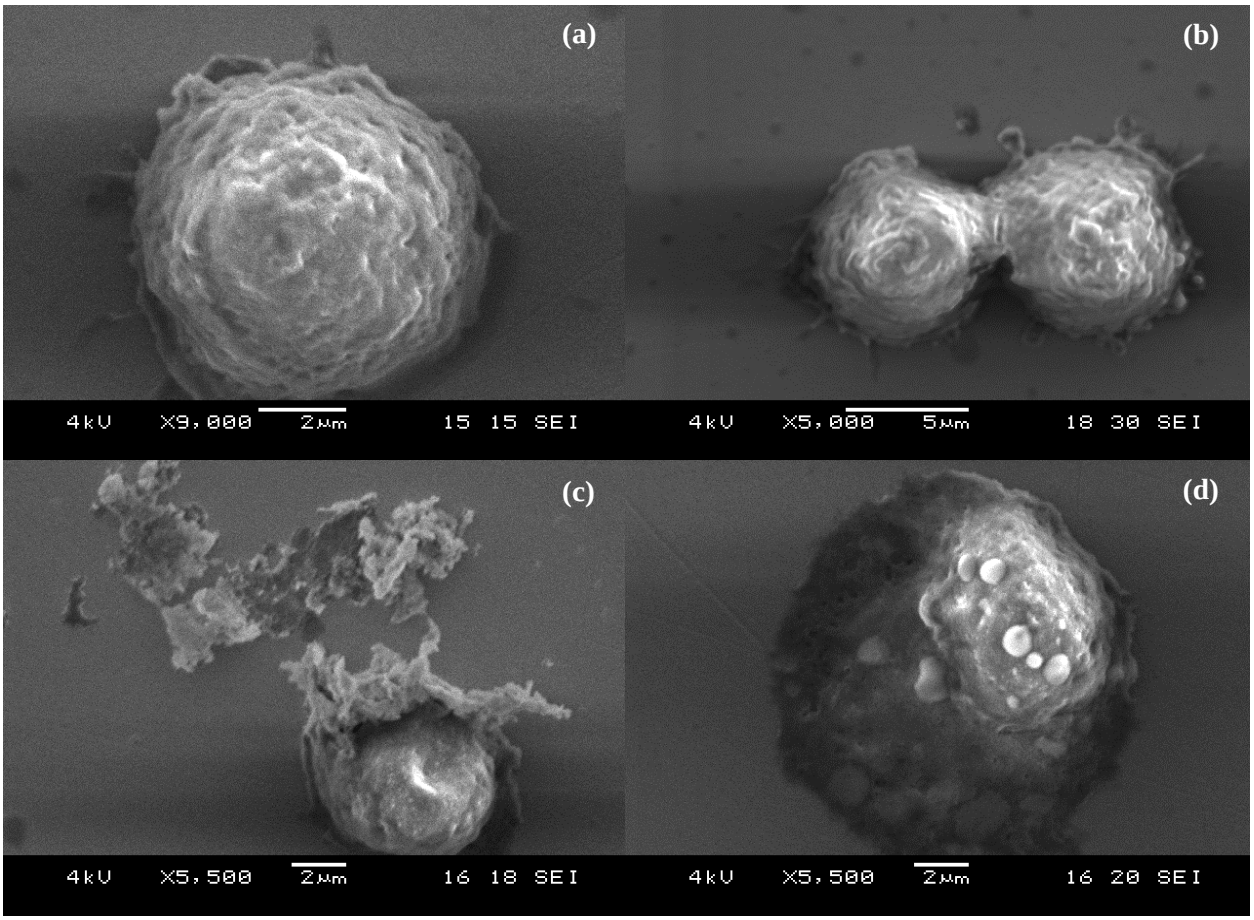

Figure 9. Matched pairs of SEM images of U937 cells on CoCrMo alloy surfaces show different cell responses to experimental conditions. Picture (a) and (b) are cells of control group (no H_2O_2 added); picture (c) and (d) are cells of 1mM H_2O_2 treatment group for 24 hours. Low kV (4 kV) was used to investigate cell membrane morphology. Cells of control group appear show intact membrane structure and cell communication. Cells of 1mM H_2O_2 treatment group show two different death mechanism based on the morphology: necrosis in picture (c), and apoptosis in picture (d).

2. Electrochemical data

2.1. Open circuit potential (OCP)

Open circuit potential data of different groups were plotted and compared in figure 10. Before all the treatments, the potential data were collected for about 30 minutes until the voltage of the whole system was relatively stable. Control group (media with/without cells) shows the OCP of CoCrMo disc was around – 0.3 V. When adding 0.25 mM H_2O_2, the potential increased to about – 0.25 V, and when adding 1 mM H_2O_2, the potential significantly increased to about + 0.25 V. After 24 hours' treatments, the potential of each group was measured again and the value all went back to around – 0.3 V which is similar to the value of control group.

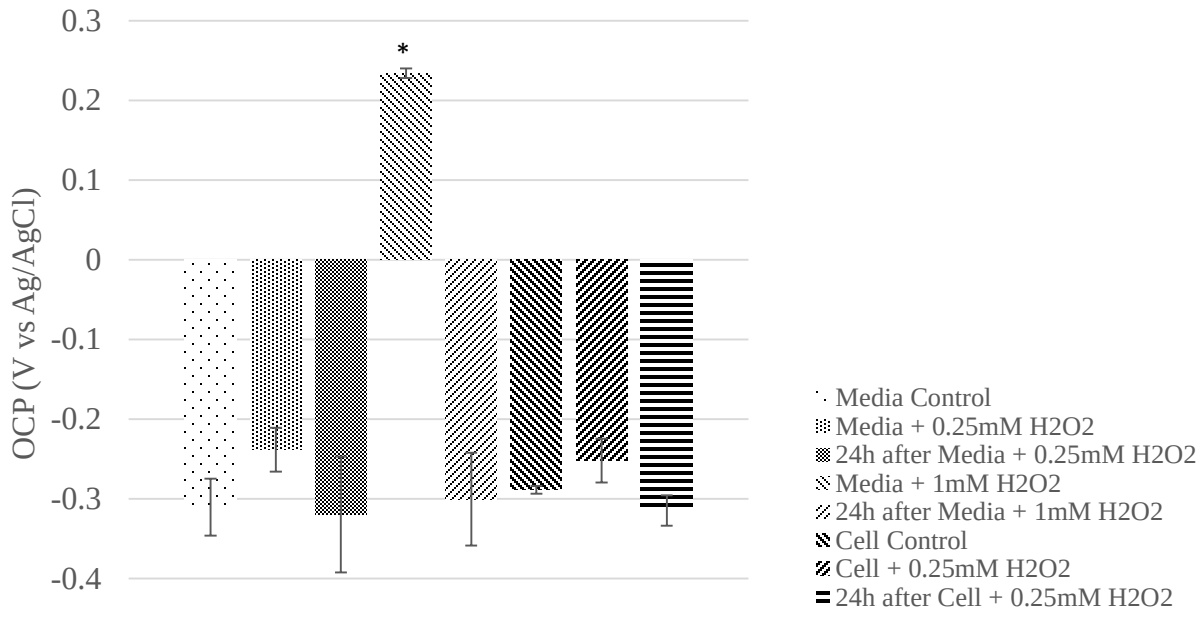

Figure 10. Open circuit potential (OCP) data of different groups before & after H_2O_2 treatment (n=3). The first column is the OCP data of CoCrMo alloy in cell culture medium before H_2O_2 treatment; the second column shows the voltage changes right after adding 0.25 mM H_2O_2 into

the medium, and the forth column is the group of 1 mM H_2O_2 treatment; the third, fifth, and eighth columns show the voltage data after 24 hours' treatment. It shows that when applying relatively high concentration of H_2O_2 (1 mM), the OCP of CoCrMo alloy will rise to positive potential.

2.2. Electrochemical impedance spectroscopy (EIS)

Electrochemical impedance testing was used to measure the corrosion resistance of CoCrMo disc under different treatment conditions. The EIS data are shown in Nyquist diagram and bode plots, the Nyquist diagram in figure 11 shows Nyquist the relationship between the real part of impedance Z' and the imaginary part Z'', notice only the 1 mM H_2O_2 treatment group shows a difference than other groups which implies a lower resistance characteristic of the system. Bode plot 1 in figure 12 shows the overall impedance data Z vs. scanning frequency, when at low frequency (0.01 Hz), |Z| value of media + 1 mM H_2O_2 group is significantly lower than other groups. Bode plot 2 in figure 13 demonstrates the relationships between the phase angle δ and scanning frequency. When phase angle is 90 degrees, the electrical behavior of an element is as a pure capacitor while when the phase angle is 0 degree, the element is a pure resistor. Other values of phase angle in between means a non-ideal capacitor behavior. In figure 13, at low scanning frequency, 1 mM H_2O_2 group shows a lower phase angle value than other groups which indicates a non-ideal capacitor behavior.

The basic impedance information were shown as Nyquist diagram and Bode plots, and more detailed electrical elements' value can be estimated if a proper circuit model can be applied. Table 6 is the summary of different electrical elements after fitting the raw data with the Randle's circuit model. Statistical data analysis showed the polarization resistance (Rp) of Media + 1 mM H_2O_2 group is significantly lower ($p < 0.05$) than other four groups and the capacitance is higher than other four groups, indicating a thinner oxide film were formed when added 1 mM H_2O_2 into the solution. And also the exponential factor α of constant phase element (CPE) of 1 mM H_2O_2 group is lower than other four groups indicating a non-ideal capacitance behavior and more defects of the oxide film.

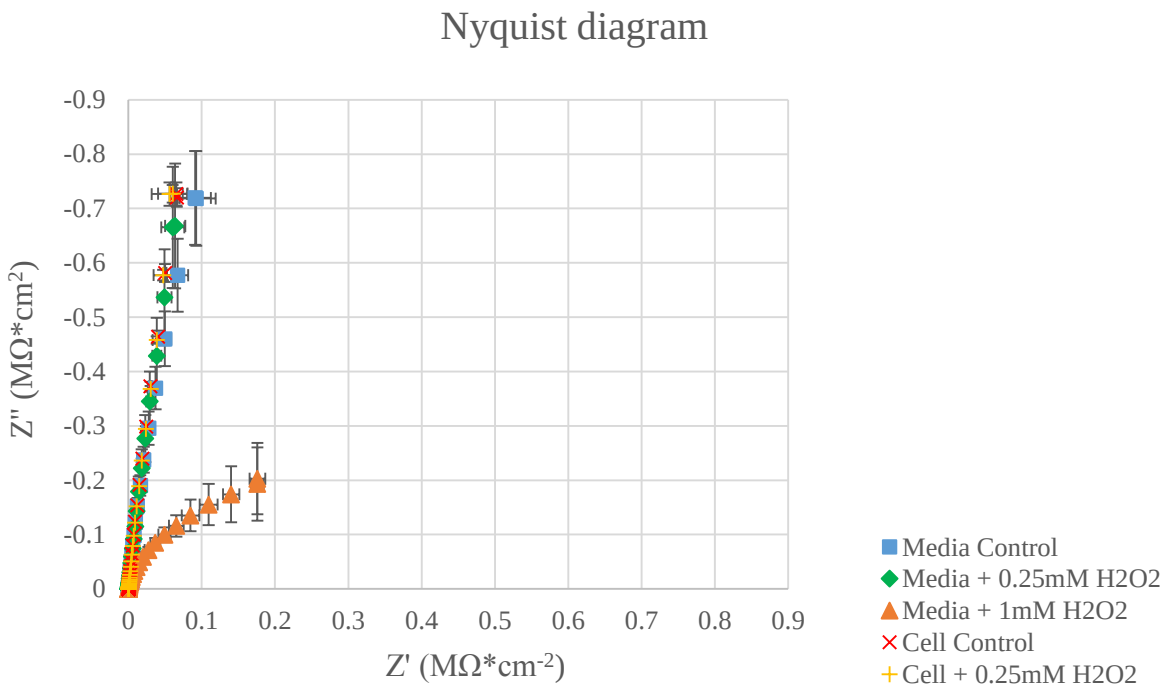

Figure 11. Nyquist diagram from electrochemical impedance spectroscopy data of CoCrMo alloy surfaces under different H_2O_2 treatment groups (n=3).

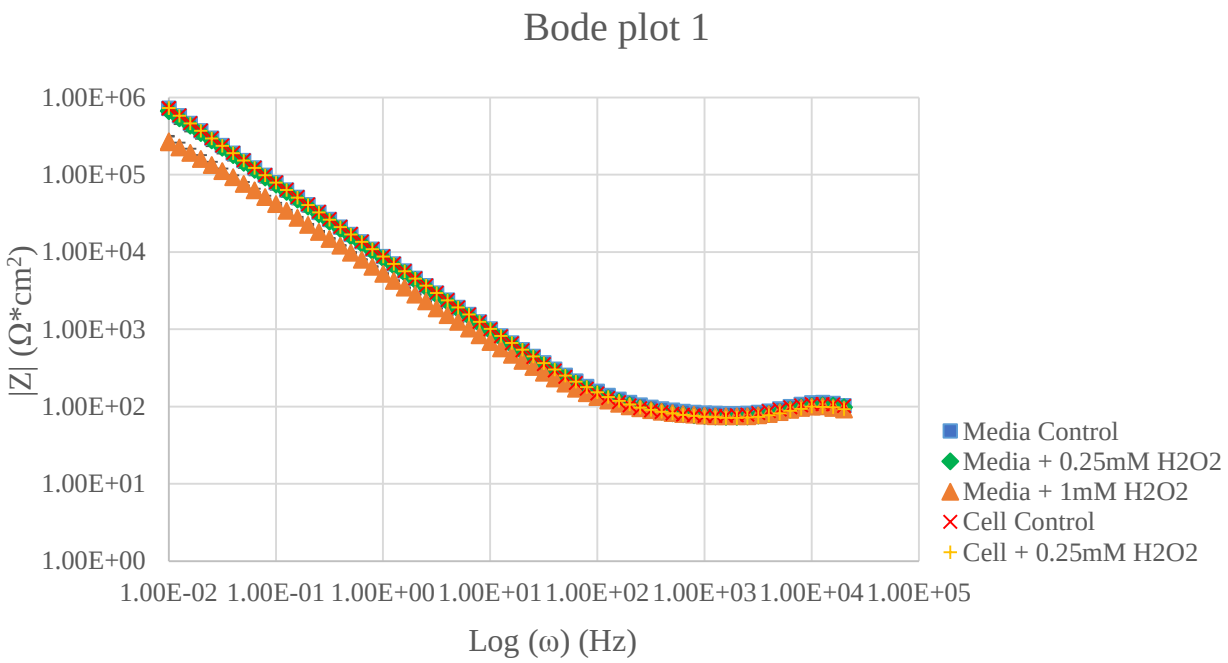

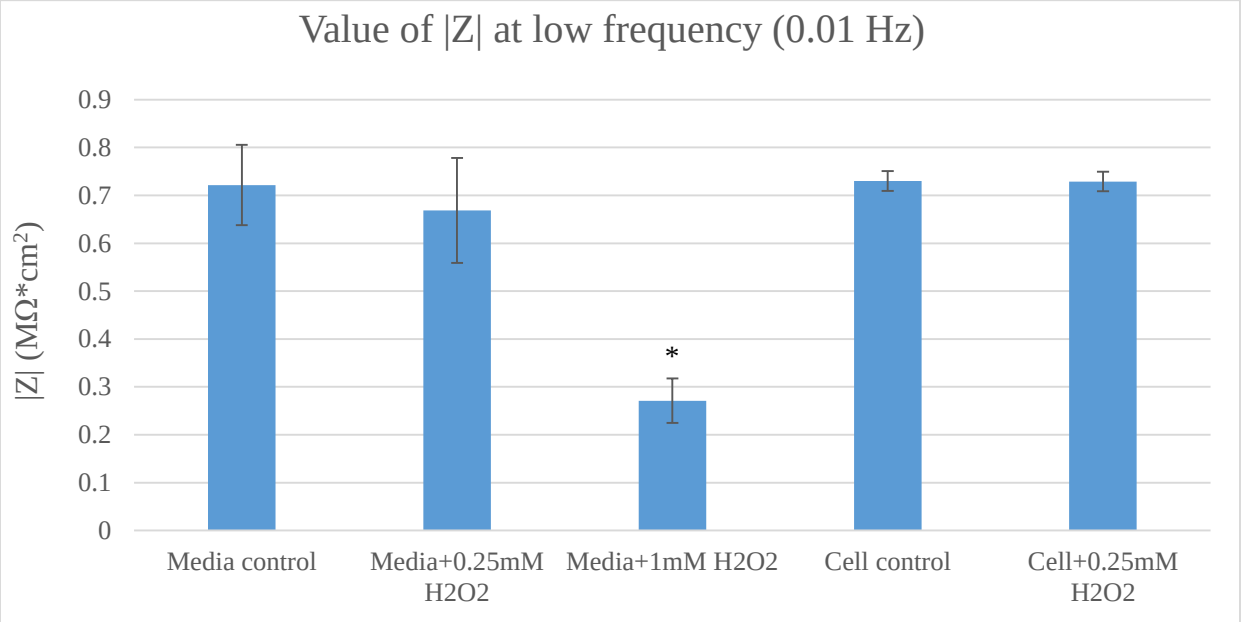

Figure 12. Bode plot 1 from electrochemical impedance spectroscopy data of CoCrMo alloy surfaces under H_2O_2 treatment groups (n=3).

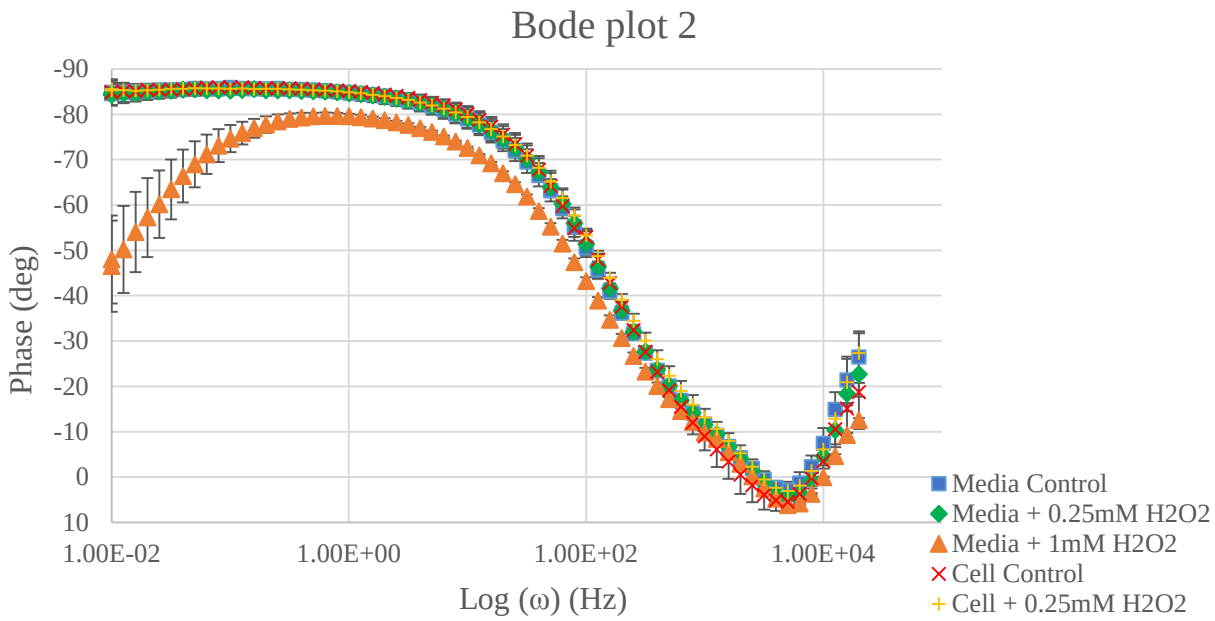

Figure 13. Bode plot 2 from electrochemical impedance spectroscopy data of CoCrMo alloy surfaces under H_2O_2 treatment groups (n=3).

Groups	Rs(Ω*cm^2)	Rp(MΩ*cm^2)	C(μF/cm^2)	α
Media	91.57 ± 2.91	17.1 ± 20.1	19.09 ± 1.56	0.945 ± 0.005
Media + 0.25 mM H_2O_2	83.92 ± 2.62	36.8 ± 101	21.30 ± 2.51	0.944 ± 0.012
Media + 1 mM H_2O_2	83.15 ± 2.02	0.493 ± 0.209	35.74 ± 0.80	0.898 ± 0.003
Cell	87.10 ± 5.20	30.1 ± 58.4	19.61 ± 0.31	0.952 ± 0.005
Cell + 0.25 mM H_2O_2	81.27 ± 5.12	38.8 ± 94.7	19.80 ± 0.12	0.944 ± 0.011

Table 6. Fitted EIS data from the Randle's circuit model. The univariate analysis shows there is a significant difference for 1 mM H_2O_2 group than other groups. The 1 mM H_2O_2 group shows a higher capacitance value and a lower polarization resistance value which indicating a thinner oxide film on CoCrMo alloy surfaces. There is also a significant difference of α, which is the exponent for constant phase element (CPE), for 1mM H_2O_2 group, the value of α is lower than other groups indicating there are more defects of the thin oxide film.

2.3. Atomic absorption spectroscopy (AAS)

The raw data of Atomic absorption spectroscopy (AAS) (Fig. 14) shows the peak values related to metal ion concentrations in solution. No peak value of Co was detected indicating the Co ion concentration was too low to be detected by the AAS machine. Figure 15 is the summary of AAS testing result, which plot (a) shows how the metal ion concentrations were acquired through voltage reading. First the standard ion solution was used to create the standard relation between voltage and concentration, then the voltage data of different samples were collected and calculated into concentration information. Figure 15 (b) shows the Cr ion concentrations in different tested groups, the values are between 6 μg/L and 8 μg/L. Based on two way ANOVA (SPSS) analysis, there is no statistical difference between groups.

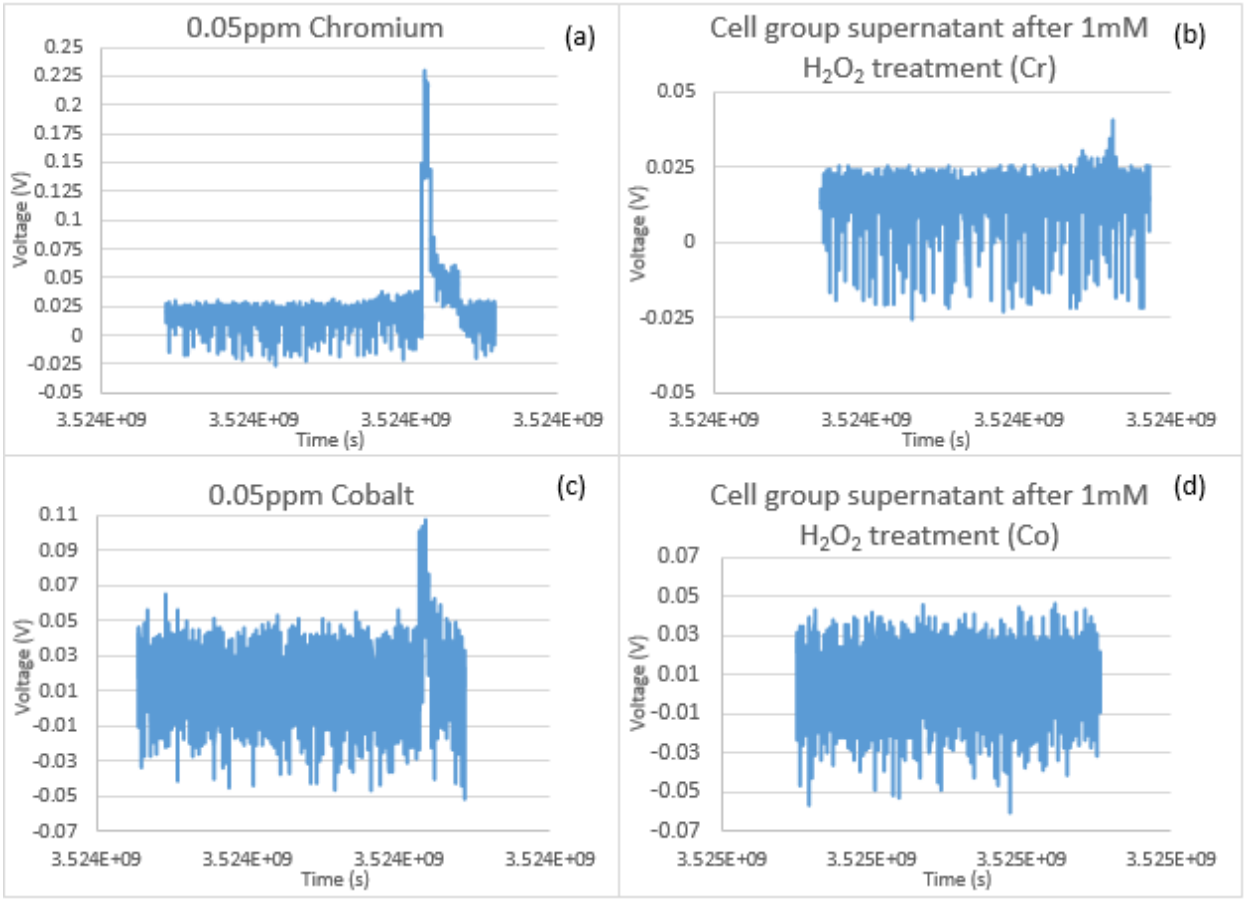

Figure 14. A series of voltage-time plots that show AAS data collected through a LabVIEW ™ program. For figure (a) and (b) the element was Cr and there is one peak for each plot, the same for figure (c). However for figure (d) there was no voltage peak within each test, the signal can't be detected because of the noise. For all the samples, only Cr can be detected but there was no Co signal shown in plots.

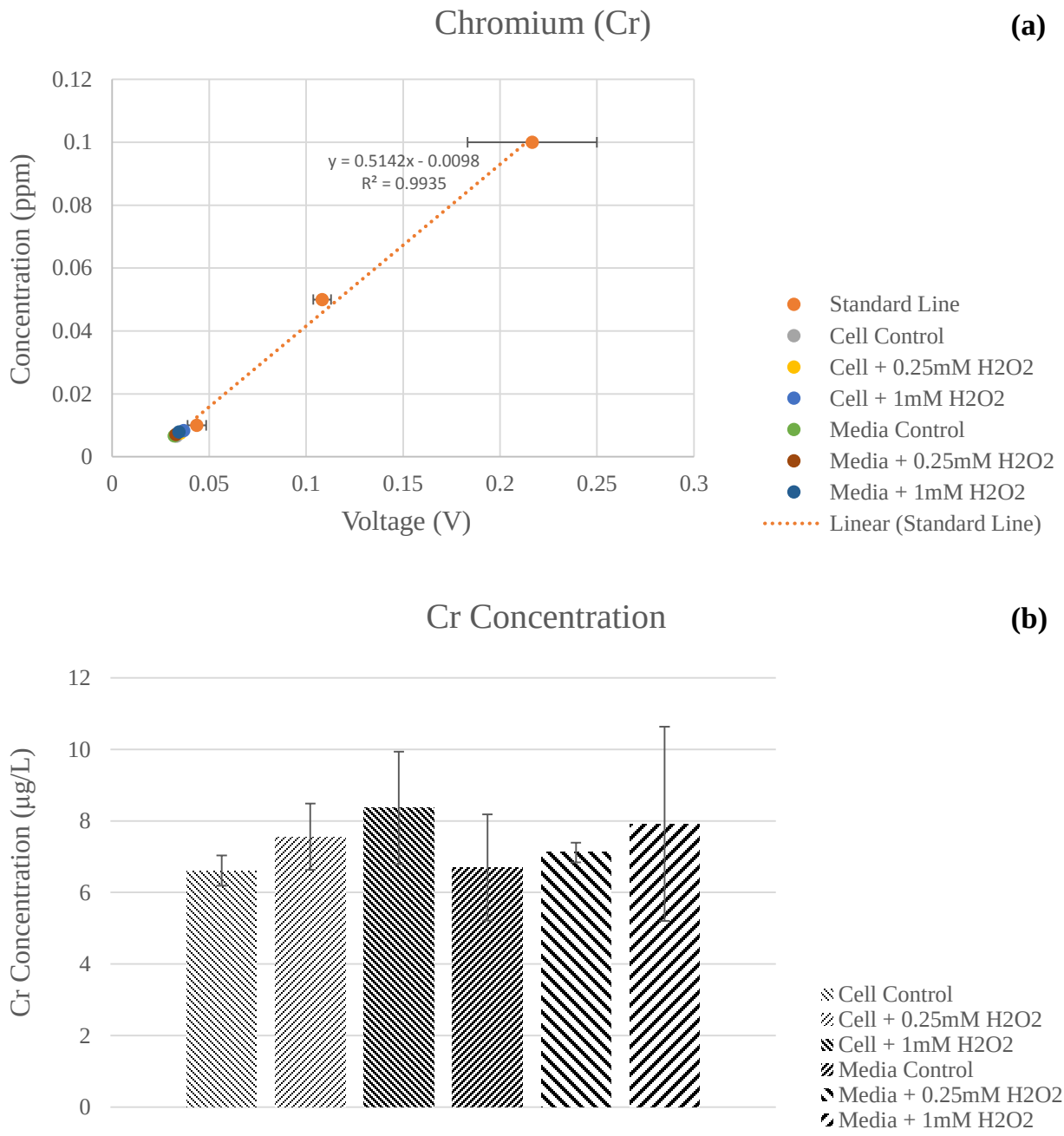

Figure 15. AAS data of all tested groups. The media samples for testing were collected after 24 hours' H_2O_2 treatment (n=3). Plot (a) shows the two standard lines acquired from standard Cr solutions (0.01, 0.05 and 0.1 ppm), based on the standard line, the Cr concentrations of all groups can be calculated from the voltage signals. Figure (b) shows the Cr concentration from 6 different groups.

Discussion

1. Cell viability and morphology

1.1. Viability

The major find of this work is that H_2O_2 kills U937 cells in a dose dependent manner and that the presence of CoCrMo increases the sensitivity of U937 cells to the killing effects of H_2O_2. In other words, the combination of metal and H_2O_2 can kill more cells than H_2O_2 alone. In the biological system, transition-metals like Cu, Fe, Co, Ti and Cr can react with H_2O_2 which is known as Fenton or Fenton-like reactions [6]. For example, Cr^{+4}/Cr^{+5} can be oxidized by H_2O_2 to form Cr^{+5}/Cr^{+6} and hydroxyl radical HO• which is recognized to be the most harmful for biological molecules [6]. For this experiment, since it used CoCrMo alloy surfaces and H_2O_2, theoretically there would be Fenton-like reactions which can produce HO• to kill more cells than H_2O_2 alone. It can be related to the *in-vivo* situations, such as post-surgery of implantation. Studies showed monocytes can differentiate into macrophages and further into phagocytes and theses cells would cover around the implant-body interfaces creating inflammation reactions [22]. The inflammatory conditions plus the presence of metal implants may trigger severe cell death and may cause aseptic loosening or bone loss.

According to the florescent images, even within the live cells under different H_2O_2 concentration treatments, they possessed different morphological shapes such as some cells were balled up spherically while some other cells can still show pseudopodia and spread cell membrane. This shows that even when cells were exposed to the same oxidative stress, some cells were still

viable and capable of functioning as macrophages. For ROS in vivo, it serves as "double-edged sword", low dose ROS can be a signaling factors or even protective of cells from apoptosis while high doses of ROS are toxic to the living system [5]. For U937 cells, studies have been performed to discover the impact of H_2O_2 on this cell line. However, there is no study of how high H_2O_2 concentration can increase *in-vivo* during inflammatory conditions. If the concentration of H_2O_2 is over a certain level that inflammatory cells can endure, it will cause damages to the host system while fighting against foreign bodies. It is important to control the inflammation reaction rate *in-vivo* to make sure it causes less damage to host body or the metal implants.

It is known that PMA treatment can induce the expression of monocytic differentiation markers CD11b and CD36 [12], and also with morphological changes such as pseudopodia. The pseudopodia characters were found both in positive control group and H_2O_2 treatment group. However, the percentage of cells with pseudopodia is different among different H_2O_2 concentration groups. Figure 8 shows the percentages of cells possessed pseudopodia from control, 0.2mM H_2O_2 and 0.3mM H_2O_2 group, although there is no significant difference between different substrates, there is a big difference between H_2O_2 treatment groups ($p < 0.05$). It clearly shows that more cells treated by 0.2 mM H_2O_2 have a higher chance to develop pseudopodia which means they are more active to perform phagocytosis. Meanwhile some studies showed that U937 cells when treated with 0.25mM H_2O_2, resulted in an induction of GPX which is a cell-expressed survival factor under oxidative stress by H_2O_2 [16]. Combining this finding with Live & Dead fluorescent pictures, 0.25 mM H_2O_2 concentration was chosen to study the impact of phagocytosis on metal-implant surfaces. Since data showed under 0.25 mM

H_2O_2, the cell viability was around 90% which means most cells can survive under this concentration and there is a high chance for cells to grow pseudopodia, meanwhile other findings [13] showed U937 cells can express relatively high level of GPX against oxidative stress. From all of the results, U937 cells not only survive but also can function as macrophages under 0.25 mM H_2O_2 concentration.

The purpose of this study was to assess the interactions between inflammatory cells and metal implant surfaces under inflammatory conditions (H_2O_2 treatment). One direction was to study the impact of implants on cells and another one was to study how cells would affect the metal implants. So a proper H_2O_2 concentration should be chosen to perform the experiments. Since there is no report about exactly how high the H_2O_2 concentration can exist around inflamed implants after Total joint arthroplasty (TJA) surgery. It's hard to predict what H_2O_2 concentration should be used to do the electrochemical tests. Based on the Live & Dead assay in this study, it showed after 24 hours cells were all dead when H_2O_2 concentration increased to 1 mM. So 1 mM was chosen to be the maximum concentration for the next experiments. Another concentration used was 0.25 mM, the reasons was based on Live & Dead result, pseudopodia percentages data and other people's studies. It shows that 0.25 mM H_2O_2 is not that toxic to U937 cells, meanwhile this concentration of H_2O_2 can serve as inflammatory signal messenger to stimulate U937 cells actively "attacking" metal implant surfaces.

A concern about the live/Dead imaging performed in this study is that when taking images of cells on CoCrMo disc, the disc has to be flipped over onto a petri-dish. Due to the gravity and

the process of handling CoCrMo disc, cell loss is inevitable especially dead cells since they are more easily come off from the CoCrMo surfaces (Fig. 7). However without considering the loss of cells for CoCrMo disc groups, the data already showed there is a significant difference of cell viability between two different culture substrate. So if considering the loss of dead cells for CoCrMo, the viability curve might be lower than what is shown in figure 5.

1.2. Morphology

The cell morphology images were shown as SEM pictures in figure 9. It is clear that when cells were treated with 1 mM H_2O_2, they were all dead according to live/dead images, however whether they die of apoptosis or necrosis can be distinguished with florescent pictures. SEM techniques were used to identify the cell death model regarding the morphological changes. In figure 9, the overall look of cells both in control and 1 mM H_2O_2 treatment group are all balled up. For 1 mM H_2O_2 treatment group, cell necrosis is readily identified by the broken membrane structure and the indentation on the cell membrane. However, for apoptotic cells, even if the membrane looks intact, there are small apoptotic bodies forming on the membrane surfaces compared to control group. This morphological finding correlates to other studies that when U937 cells are exposed to 1 mM H_2O_2, both apoptosis and necrosis can occur and cause cell death [17].

2. Electrochemical study

For the electrochemical tests, OCP, EIS and AAS were performed to study the changes of metal surfaces of all the groups.

2.1. Voltage data

For the cell seeding density used in this study (20,000 cells/3.8 cm^2), there was no difference in OCP between cells on the metal disc or not (Fig. 10). Even when cell seeding density was increased to 200,000 cells/3.8 cm^2 (data not shown). The OCP data shows H_2O_2 played an important role however the inflammatory cells didn't show a significant impact. It is obvious that when 0.25 mM H_2O_2 concentration treatment was used, the voltages only rose from around -0.3 V to -0.25 V (vs. Ag/AgCl). When treating the metal disc with 1 mM H_2O_2, the voltage would increase from negative -0.3 V to positive around 0.25 V (vs. Ag/AgCl) which indicates the equilibrium of oxidation reaction and reduction reactions were shifted significantly to a higher oxidizing condition. The rise of OCP indicates that the CoCrMo oxide film was impaired so the alloy itself tended to form a new oxide film to the passivation zone. And because of the new oxide film forming, the anodic currents dominate which cause the rise of the OCP. And according to this experimental design, there was no constant and stable H_2O_2 supplement to hold the concentration around 1 mM, all the data were collected immediately after adding H_2O_2 since H_2O_2 is unstable and easily undergoes dismutation reaction into H_2O and O_2. However *in-vivo* if there is inflammation especially after arthroplasty surgery, the H_2O_2 concentration would be stable and would last for a long time to affect the performance of prosthesis. Even this study was

not a long term trial, but it can still predict how metal would be affected by the rise of ROS species (especially H_2O_2) *in-vivo*.

Another finding regarding the OCP data is that when added 1 mM H_2O_2, the voltage increased to + 0.25 V and then decreased back to around – 0.3 V after 24 hours. This indicates after 24 hours, the effect of H_2O_2 on CoCrMo OCP was gone, it might be either because of the dismutation reaction ($H_2O_2 – H_2O + O_2$) or because of the presence of CoCrMo which might accelerate the consumption of H_2O_2. To investigate this hypothesis, extra experiments need to be done in the future and tested groups should be H_2O_2 with/without CoCrMo presence, and measure the H_2O_2 concentrations vs. time.

2.2. Impedance data

According to the impedance data, inflammatory cells did not affect impedance properties. Like the data shown before, only when 1 mM H_2O_2 solution was used was there a great decrease of impedance from 10E+7 $\Omega*cm^2$ to 10E+5 $\Omega*cm^2$ (see Table 6). At lower frequencies, 1 mM H_2O_2 group showed lower phase angle which indicated the metal surface was like a non-ideal capacitor interface behavior since phase angle of 90 degree means an ideal purely capacitive character. Based on all the information, the conclusion can be drawn that when H_2O_2 concentration reaches a certain level, the metal oxide surface will start to change losing its barrier properties and making it easier for electrons or ion transferring through the interface. This means the metal will be more susceptible to corrosion. One hypothesis before this experiment

was that when macrophages were activated, based on their functioning, they will try to generate chemicals and cytokines such as ROS species, acids, IL-1 etc. to attack the metal implant surfaces. The purpose of studying the metal impedance was to investigate whether the activated macrophages will affect the impedance behavior of metal surfaces. However the data showed no differences between control group and activated U937 cell group. The possible explanations could be low cell seeding density (5,300 cells/cm^2), short term treatment (24 hours) or the large area of the electrode (3.8 cm^2). For the cell seeding density, a higher cell density (53,000 cells/cm^2) was tried with the same treatment period (24 hours). Nevertheless no changes in impedance was observed. Another consideration of EIS study of cells on metal surfaces is that when cells are adherent to metal surfaces, the impedance data is not solely from metal but also from cell membrane. For later study, a micro-electrode could be designed to investigate the impedance of a single cell covered metal surface area.

2.3. AAS data

AAS test is to measure specific metal ions concentration in solutions. In this study the media solutions were all collected after OCP and EIS tests for the AAS measurements. Cr and Co ion concentrations were tested, however due to the machine compliance, the noise of detecting Co concentration was too high that no signal of Co can be captured in all tested media. Only Cr ions signals can be detected.

Even though after two way ANOVA (SPSS) analysis there is no significant difference between tested groups, however there is an apparent tendency of higher metal ion levels with H_2O_2 treatment. A limitation of this experiment was that the media was collected only after 24 hours treatment limiting the level of ions released into solution. Meanwhile referring to N. Muhamad et al., they collected media after around 2 weeks or longer time to measure the ion release behavior of metal implants [24]. Therefore long-term experiments are needed to study how inflammatory conditions may affect metal ion dissolution from implants. Despite there being no significant difference between control and H_2O_2 treated groups, it is clear that the metal implants can release ions into the surrounding solutions according to other researchers' works and this study (6 – 8 µg/L). Based on the Fenton reaction theory, transition metal ions such Cr^{+3}/Cr^{+6} can react with H_2O_2 to form hydroxyl radicals HO• which possess the most toxic effects towards biological molecules [6]. This might explain why U937 cells exhibited lower viability when treated with the same H_2O_2 concentration on CoCrMo disc then on 6 well plate.

Conclusion

- H_2O_2 as an oxidative stress element can do more damage to U937 cells cultured on CoCrMo alloy disc surface than cells cultured on 6 well plates.
- Low concentration of H_2O_2 treatment (0.2 mM) can trigger U937 cells to develop pseudopodia which is a sign of activated macrophages when compared to control groups.
- Relatively high concentration of H_2O_2 (1 mM) can cause the potential increase of CoCrMo alloy and defects of CoCrMo alloy surface oxide film. CoCrMo alloy would be more susceptible to corrosion under inflammatory conditions.

Future work

According to this study, the weakest point is that it is a short term experiment (only 24 h treatment) which couldn't fully explain how metal implants would be affected by inflammatory conditions and inflammatory cells. According to this concern, the first idea of improving the chemical chamber system is to add a pump which can continuously supplying H_2O_2 into the media to maintain the H_2O_2 concentration as constant oxidative stress for long term study of metal implants and cells interaction. Since the H_2O_2 can raise the metal implants potential to certain level, it can be an indicator to adjust the frequency of pumping H_2O_2 (for example, if the potential can be raised to +200 mV, just adjust the frequency of the pump to keep the potential around +200 mV which can indirectly indicate that the H_2O_2 concentration is steady).

Another idea of studying metal implants' performance *in-vitro* is to combine fretting test with oxidative stress. As it is agreed that one of the most common causes of metal implant failure is due to fretting corrosion, since modernized metal implants are all made of modular parts which micro-motions between parts are inevitable. Another concern been found and published by Gilbert et al. that there is a strong evidence of inflammatory cell induced corrosion found on the surfaces of CoCrMo alloy implants [23]. So considering the situation of after arthroplasty surgery, there would be a fretting area surrounded by inflammatory fluid and cells which might cause an early stage implant failure. Due to this concern, an *in-vitro* study of fretting corrosion under inflammatory fluid with inflammatory cells would be profound and if the mechanism can be discovered, better design of metal implants can be created to reduce the failure of metal implants.

Inflammation is always an important topic in biomedical filed. Since it can not only cleaning the wounded area, but also can do more damage to host system. Now studies also showed inflammation might also be a vital reason of implant failure. So understanding how to control inflammation reaction after implant surgery is promising both for implant long last in human body and relieving the pain from inflammation. For future study, if the voltage of metal implants can be brought down to lower value during inflammation reactions after surgery, more electrons can be available on metal surfaces to consume more ROS species. Hence severe inflammatory conditions can be controlled to mild level that will cause less damages either to host body or implant.

References

1. Hendra H, Dadan R, R.P DJ. Metals for Biomedical Applications. *Biomed Eng - From Theory to Appl*. 2011:411-431.

2. Chen Q, Thouas G a. Metallic implant biomaterials. *Mater Sci Eng R Reports*. 2015;87:1-57.2014.10.001.

3. Ehrensberger MT, Sivan S, Gilbert JL. Titanium is not "the most biocompatible metal" under cathodic potential: The relationship between voltage and MC3T3 preosteoblast behavior on electrically polarized cpTi surfaces. *J Biomed Mater Res - Part A*. 2010;93(4):1500-1509.

4. Kim J, Gilbert JL. Cytotoxic effect of galvanically coupled magnesium-titanium particles. *Acta Biomater*. 2016;30:368-377.

5. Martin KR, Barrett JC. Reactive oxygen species as double-edged swords in cellular processes: low-dose cell signaling versus high-dose toxicity. *Hum Exp Toxicol*. 2002;21(2):71-75.

6. Prousek J. Fenton chemistry in biology and medicine. *Pure Appl Chem*. 2007;79(12):2325-2338.

7. Wittmann C, Chockley P, Singh SK, Pase L, Lieschke GJ, Grabher C. Hydrogen peroxide in inflammation: Messenger, guide, and assassin. *Adv Hematol*. 2012;2012.

8. Loo AEK, Wong YT, Ho R, et al. Effects of Hydrogen Peroxide on Wound Healing in Mice in Relation to Oxidative Damage. *PLoS One*. 2012;7(11).

9. Harris P, Ralph P. Human leukemic models of myelomonocytic development: a review of the HL-60 and U937 cell lines. *J Leukoc Biol*. 1985;37(4):407-422.

10. Ratner BD, Hoffman AS, Schoen FJ, Lemons JE. *Biomaterials Science: An Introduction to Materials in Medicine*.; 2004.

11. Yamamoto T, Sakaguchi N, Hachiya M, Nakayama F, Yamakawa M, Akashi M. Role of catalase in monocytic differentiation of U937 cells by TPA: hydrogen peroxide as a second messenger. *Leuk Off J Leuk Soc Am Leuk Res Fund, UK*. 2009;23(4):761-769.

12. Hass R, Bartels H, Topley N, et al. TPA-induced differentiation and adhesion of U937 cells: changes in ultrastructure, cytoskeletal organization and expression of cell surface antigens. *Eur J Cell Biol*. 1989;48(2):282-293.

13. del Bello B, Paolicchi a, Comporti M, Pompella a, Maellaro E. Hydrogen peroxide produced during gamma-glutamyl transpeptidase activity is involved in prevention of apoptosis and maintainance of proliferation in U937 cells. *FASEB J*. 1999;13(1):69-79.

14. Burdon RH. Superoxide and hydrogen peroxide in relation to mammalian cell proliferation. *Free Radic Biol Med*. 1995;18(4):775-794.

15. Tang D, Shi Y, Kang R, et al. Hydrogen peroxide stimulates macrophages and monocytes

to actively release HMGB1. *J Leukoc Biol*. 2007;81(3):741-747.

16. Lee BR, Um HD. Hydrogen peroxide suppresses U937 cell death by two different mechanisms depending on its concentration. *Exp Cell Res*. 1999;248(2):430-438.

17. Palomba L, Sestili P, Columbaro M, Falcieri E, Cantoni O. Apoptosis and necrosis following exposure of U937 cells to increasing concentrations of hydrogen peroxide: the effect of the poly(ADP-ribose)polymerase inhibitor 3-aminobenzamide. *Biochem Pharmacol*. 1999;58(11):1743-1750.

18. Cerella C, Coppola S, Maresca V, De Nicola M, Radogna F, Ghibelli L. Multiple mechanisms for hydrogen peroxide-induced apoptosis. *Ann N Y Acad Sci*. 2009;1171:559-563.

19. Muhamad Wahab NB, Abdul Majid FA, Abdul Kadir MR. Toxic element released from high and low carbon CoCrMo alloy in-vitro. *Proc 2010 IEEE EMBS Conf Biomed Eng Sci IECBES 2010*. 2010;(December):180-183.

20. Campbell JR, Estey MP. Metal release from hip prostheses: Cobalt and chromium toxicity and the role of the clinical laboratory. *Clin Chem Lab Med*. 2013;51(1):213-220.

21. Dayan a D, Paine a J. Mechanisms of chromium toxicity, carcinogenicity and allergenicity: review of the literature from 1985 to 2000. *Hum Exp Toxicol*. 2001;20(9):439-451.

22. Scharf B, Clement CC, Zolla V, et al. Molecular analysis of chromium and cobalt-related toxicity. *Sci Rep*. 2014;4

23. Gilbert JL, Sivan S, Liu Y, Kocagöz SB, Arnholt CM, Kurtz SM. Direct in vivo inflammatory cell-induced corrosion of CoCrMo alloy orthopedic implant surfaces. *J Biomed Mater Res - Part A*. 2014:211-223.

24. N. Muhamad Wahab, F. Abdul Majid, M. Abdul Kadir. Toxic element released from high and low carbon CoCrMo alloy in-vitro. *Proceeding of 2010 IEEE EMBS Conference on Biomedical Engineering and Sciences, IECBES 2010.*

Vitae

Huiyu Shi

126 Jamesville Ave. Apt. R4, Syracuse NY 13210
Cell: 315-515-1770. Email: hshi12@syr.edu

Summary

- Biomedical engineer with 3 years of experiences in biomaterials and tissue engineering.
- Expertise in wide range of cell culturing techniques and electrochemical testing methods.
- Skilled in various laboratory equipment, such as digital optical microscopy, SEM, EDS, AAS, and FTIR.
- Able to utilize engineering software, such as Image J, LabVIEW, AutoCAD, and SPSS.
- Knowledgeable in PCR, ELISA, Southern blot, SDS-PAGE, Western blot and transfection.
- Proficient in oral and written communication skills.

Education

M.S. in Biomedical Engineering at Syracuse University, Syracuse, NY (August 2013 – May 2016)

GPA: 3.667/4.0.
Thesis Title: "Interactions between Inflammatory Cells and CoCrMo Alloy Surfaces under Simulated Inflammatory Conditions".
Thesis Advisor: Dr. Jeremy L Gilbert.

B.S. in Biological Sciences at Wuhan University, Wuhan, Hubei Province, China (September 2006 – June 2010)

GPA: 3.0/4.0.
Thesis Title: "The Preliminary Study of PPM1B Eukaryotic Expression Vector pCMV-Tag2B's Construction and Function".
Thesis Advisor: Dr. Ying Zhu.

Research Experience

Research Assistant, M.S. (August 2013 – May 2016)
Syracuse Biomaterials Institute, Syracuse University, Syracuse NY

- Investigated the cytotoxicity of oxidative stress of macrophages cultured on CoCrMo alloy surfaces and tissue culture substrate. Used Live/Dead (fluorescence) imaging, digital optical microscopy, and SEM to measure cell viability and cell morphology.

- Studied the electrochemical behavior of CoCrMo alloy surfaces under simulated inflammatory conditions (H_2O_2 + inflammatory cells). Measured OCP and impedance using Solartron potentiostat. Measured metal ion concentrations using AAS.

Research Assistant, B.S. (September 2006 – June 2010)
State Key Laboratory of Virology, Wuhan University, Wuhan, Hubei Province, China

- Studied transfection of PPM1B gene into human embryonic kidney cells. Used RT-PCR to amplify PPM1B DNA sequences from extracted RNA, then inserted into competent *E.Coli* plasmid, the plasmid vector was then introduced into human embryonic kidney cells. Used SDS-PAGE and Western blot technique to quantitatively investigate the expression of PPM1B protein in the kidney cells.

- Another study involved investigating the effect of different chemicals (lipopolysaccharides, TNF-α, and IFN-γ) induced inflammatory pathway (cyclooxygenase-2) in human peripheral blood mononuclear cells (PBMC) by using ELISA technique.

Work Experience

Internship (September 2010 – July 2012)
Center for Disease Control and Prevention, Xiantao, Hubei Province, China

- Investigated contaminated samples (i.e. food, water) and distinguished what kind of microorganisms (bacteria, fungi etc.). Collaborated with other departments to cure the contamination.

Skills

Experimental Skills:

- Cell culture (mammalian & bacterial)
- Live/Dead viability assay
- Digital optical microscopy
- SEM & EDS
- AAS
- FTIR
- Electrochemical testing
- PCR
- ELISA
- SDS-PAGE
- Southern blot & Western blot

Computer Skills:

- Microsoft Word, Excel, and PowerPoint
- LabVIEW
- Image J
- AutoCAD
- SPSS Statistics

Language Skills:

- English – Proficient
- Chinese – Native

Conference Presentations/Posters

- **Shi H** and Gilbert JL. "Interactions between Inflammatory Cells and CoCrMo Alloy Surfaces under Simulated Inflammatory Conditions." Stevenson Lecture, Syracuse University, Syracuse, New York; March 2016.